Regional Studies in Marine Science 16 (2017) 1–14

Contents lists available at ScienceDirect

Regional Studies in Marine Science

journal homepage: www.elsevier.com/locate/rsma

Tidal impact on suspended sediments in the Macuse estuary in Mozambique

Lucas Lavo António Jimo Miguel [a,b,c,*], João Wagner Alencar Castro [a,c], Fialho Paloge Juma Nehama [b]

[a] Programa de Pós-graduação em Geologia PPGl–UFRJ, Brazil
[b] Escola Superior de Ciências Marinhas e Costeiras –ESCMC/ Universidade Eduardo Mondlane, Mozambique
[c] Laboratório de Geologia Costeira, Sedimentologia e Meio Ambiente - LAGECOST / Museu Nacional–UFRJ, Brazil

HIGHLIGHTS

- The tidal regime of 4 m in height generates tidal currents of 120 cm s^{-1} between the ebb and flood tides.
- Silt sedimentation occurred with 0.10 cm s^{-1} and fine sand was found to be 10 cm s^{-1}.
- Besides tidal currents, runoff discharge and wind energy has controlled the mixing in both rainy and dry seasons.
- The observed and predicted sediment indicated silt concentration of 300 mg l^{-1} in rainy season and 200 mg l^{-1}in dry season.

ARTICLE INFO

Article history:
Received 17 December 2016
Received in revised form 5 July 2017
Accepted 8 July 2017
Available online 26 July 2017

Keywords:
Tidal currents
Suspended sediments
Sedimentation
Macuse Estuary

ABSTRACT

Many studies around the world have found that tidal dynamics control the transport of suspended sediments in estuaries, as well as their relationship with runoff discharges and bathymetry morphology. This manuscript examines tidal impact on suspended sediments in the Macuse estuary in Mozambique, southern Africa. Data was collected at 42 stations, including tidal current measurements with an Acoustic Doppler Current Profiler (ADCP), tide elevation with a tidal gauge and suspended sediments with a Niskin bottle. A 14-month model simulation was implemented beginning in November 2013, forced by tides, wind regime and runoff discharges. The results indicated a tidal elevation of 4 m that generated tidal currents of 120 cm s^{-1}. These currents combined with the runoff of 500 m^3 s^{-1} and bathymetry configuration, drove the suspended sediments during the ebb and flood tides. Suspended sediment concentrations suggested the occurrence of sedimentation where water flow was less than 0.10 cm $s^{-1}$for silt and less than 10 cm s^{-1} for fine sand. Results of silt concentrations was about $\sim$ 300 mg l^{-1} while fine sand was found to be 0.2 mg l^{-1}in both tidal periods in ebb and flood tides during the rainy and dry seasons. The model accuracy of about R^2 = 0.88 between the observed and simulated results demonstrated the ability to predict the impact of tides and runoff discharges in the Macuse estuary and may be extended to other estuaries. The model matches in reproducing the sediment transport mechanism will help making political decisions about the estuary sustainability and local coastal management.

1. Introduction

Estuaries at land–sea interfaces are critical to the functioning of coastal systems. Their dynamics are caused primarily by a combination of tidal elevation and storm surges, changes to the wave climate, and high runoff discharges which intensify during rainy seasons (Quinn et al., 2014). Estuarine flooding or ebbing caused by tidal elevation combined to storm surge and to extreme river flow can increase flood hazards in many estuaries (Maskell et al., 2013). Tidal elevation and runoff discharges may change daily and seasonally, increasing flood risk, intensifying tidal current dynamics, tidal asymmetry and the supply of suspended sediments. The sediment supply can produce highly productive environments that may serve as important routes through which terrestrial material enters into the ocean (Simpson et al., 2001). These materials are highly influenced by environmental dynamics that change their sedimentological, chemical and biological structure in different spatial and temporal scales (Valle-Levinson, 2010). Many studies confirm that these changes may be caused by the combination of

* Correspondence to: Laboratório de Geologia Costeira, Sedimentologia e Meio Ambiente - LAGECOST / Museu Nacional–UFRJ, Brazil. Quinta da Boa Vista, s/n, São Cristovão, CEP. 20940-040, Rio de Janeiro
E-mail address: lucaslavomiguel@ufrj.br (L.L.A.J. Miguel).

http://dx.doi.org/10.1016/j.rsma.2017.07.002
2352-4855/

tidal dynamics and runoff discharges that control the transport of suspended sediments and their morphology.

Several studies have indicated that potentially negative impacts of estuarine changes caused by tidal changes and river flooding might include, sediment supply that may damage infrastructure and population displacement (Hanson et al., 2011; Nicholls et al., 2011), increased erosion and loss of land to the sea (Zhang et al., 2004), pollution and increased human health risk, and significant loss of wetland habitats and ecosystems (Day et al., 1995; Nicholls et al., 1999). In this case, any modeling process involving environmental factors might bring output results into questions. Different researches about the impact of tides on the dynamic of suspended sediments in estuaries are found around the world (Biggs, 1970; Gelfenbaum, 1983; Fain et al., 2001; Patchineelam and Kjerfve, 2004; Grabemann and Krause, 2001) in which the principles were extended to the East coast of Africa (Liu, 2014; Kitheka et al., 2005; Nehama, 2012; Chevane et al., 2016; Maskell et al., 2013; Van der Lubbe et al., 2014). These studies analyzed the importance of developing modeling approaches to predict suspended sediments, water discharges and tidal flooding risk, which will help assess impacts and support mitigation decisions for port construction.

Decadal increase of suspended sediment supply from both the river and sea may cause depth changes and flood risk due to the lower depths caused by sediment deposition over long time scales (Miguel, 2013). Specifically in East Africa, Liu (2014), Kitheka et al. (2005), Nehama (2012) and Chevane et al. (2016) provided various results of coastal processes in the region and have helped provide better understanding of tidal dynamics and runoff discharges. The effect of these factors on suspended sediments modifies not only estuary morphology but also light penetration as well as affects navigability and harbor logistics. Meanwhile, there is no studies in Mozambique that have focused on the impact of tidal elevation and river discharges on suspended sediments in estuaries strongly dominated by tides. This study examines the impact of tides on suspended sediments at the Macuse estuary in Central Mozambique, where is located a harbor with regional strategic importance for central Mozambique and landlocked countries in the interior.

1.1. Study site

Located in Zambezia Province in central Mozambique, the Macuse river estuary serves as one of the major outlets for discharge of Namacurra River runoff, which is estimated to average 500 $m^3\ s^{-1}$ during the rainy season (Fig. 1). The Macuse floodplain has been used for rural development, particularly rice cultivation and a recent port project by the Mozambican government. Intensification of agriculture and the port project may increase sediment supply to the Namacurra River as well as alter its tidal regimes and thus cause immense changes in the bathymetry of the river channel.

Previous studies find that the combination of transgressions and regressions and the sediment supply have formed several tidal plains characterized by beaches with very fine and fine sand and several mangrove fields that extend up to about 40 km inland to the Namacurra district. These fields are composed of several species of typical mangrove vegetation and an abundance of very fine material (mud, clay and silt), and are colonized by populations of benthos and molluscs.

Moore et al. (2008) state that the regional climate is tropical humid according to the Köppen scale and is affected by the warm Mozambique current. This current has a strong effect on the annual seasons according to studies by Ramsay (1995), Armitage et al. (2006), Halo et al. (in press) and Lutjeharms and van Ballegooyen (1988). Two annual seasons are quite evident in the region—summer from September to March and winter from April to August. Annual rainfall averages roughly 1000 mm $year^{-1}$ with annual average temperatures of 24 °C (Moore et al., 2008). Maximum rainfall and Macuse riverine runoff occur during the austral summer between January and March when the Intertropical Convergence Zone (ITCZ) and associated rainfall belts reach their southernmost position (Moore et al., 2008). The rainfall have fed runoff discharges that reach maximum discharges of 800 $m^3\ s^{-1}$ between February and March.

The region has weak nebulosity and prevailing winds from the east and the southeast. The monthly 10 m winds vary between 3.5 m s^{-1} and 5.5 m s^{-1} with the predominating frequencies being from the NE, E, SE, S and SW (Langa, 2007; Miguel, 2013). Although the wind intensities are relatively weak, the local winds are the main factor responsible for generating waves averaging 1.5 m in height. The wave regime is predominantly from the southeast and is influenced by SE winds that generate the south–north longshore water current (Lutjeharms and van Ballegooyen, 1988). This longshore water current is responsible for the sediment transportation and coastal hydrodynamic circulation along the Mozambique coastline. According to the National Institute of Hydrography and Navigation of Mozambique—INAHINA (2013), the region has a tidal range of about 4 m during spring tides, which generates tidal currents of about 120 cm s^{-1}, that may cause erosion and transport of particulate suspended sediments.

2. Materials and methods

2.1. Synoptic data collection

We set up locations of 42 stations along the estuary that were identified in the field with GPS-Garmin, to get correct coordinates on the base map. The stations were selected to ensure greater coverage of the study area, determining longitudinal and transversal vertical sections. In November 2013 and November 2014, was conducted a field survey with CTD profilers (conductivity, temperature and depth sensors) and a tidal gauge to collect synoptic data, including water temperature, tidal currents, tidal elevation, water salinity, suspended sediments and water turbidity. Salinity units are in PSU or g kg^{-1}, however in this research have been considered unitless. Suspended sediments were measured by sampling 3.5 liters of water in a Niskin bottle. The collected sediments were filtered using 0.47 μm porosity fiberglass, 0.45 mm in diameter.

The meteorological data (from 2000 to 2013) were acquired from the National Meteorological Institute of Mozambique (INAM), which routinely collects precipitation, air temperature and their derivatives at a dense network of stations. Hydrological data were acquired from the National Water Directorate of Mozambique for the period between 2000 and 2013 at the Licungu River at station 91 in Mocuba district, which continuously records water heights.

2.2. ELCOM module

The Estuary Lake and Coastal Ocean Model (ELCOM) was developed at the University of Western Australia. ELCOM is a numeric model that uses thermodynamic and hydrodynamic principles to simulate the spatial and temporal variations of physical, chemical, biological, and geological parameters in natural water bodies. This particular model was chosen because studies by Hipsey and Hamilton (2008), Miguel (2013), Hodges and Dallimore (2013), Hodges and Dallimore (2007) and Hodges et al. (2000) have found that ELCOM is a strong and reliable tool for predicting physical, biological and chemical parameters.

Indeed, the ELCOM model is a tool used to predict oceanographic parameters in natural water bodies subjected to external environmental forces. These environmental forces are usually wind stress, tides, precipitation, surface heating or cooling as well as inflows and outflows of water. The model uses hydrostatic

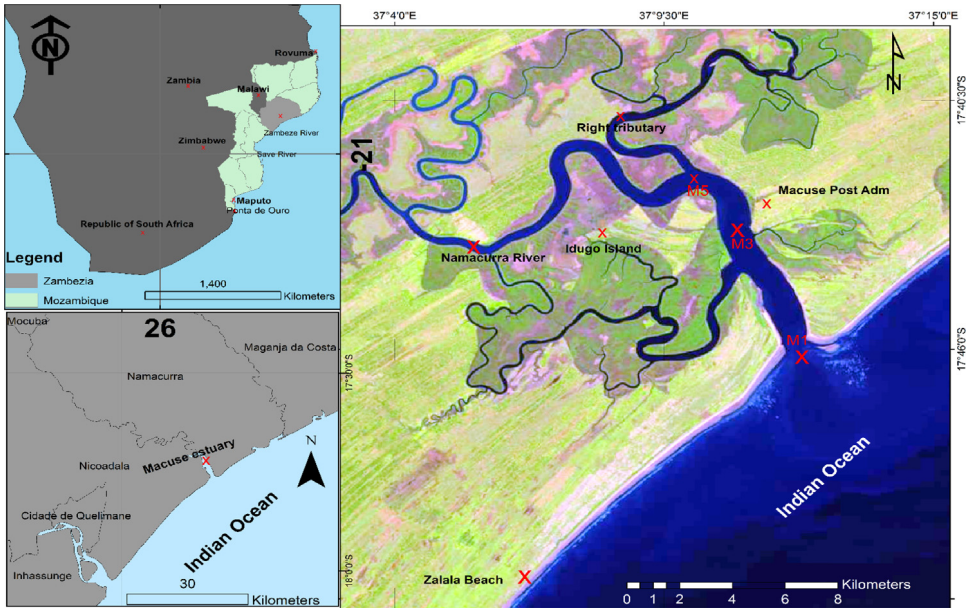

Fig. 1. Macuse estuary within the context of southeast Africa in Mozambique. M1 is the entrance boundary, while the Namacurra River and right tributary are the upstream boundaries.

pressure assumptions based on the Navier–Stokes equations for incompressible flow (Hodges and Dallimore, 2007). Besides the hydrostatic assumption for pressure, the Boussinesq approximation and Reynolds averaged transport equations (1)–(3) are implemented (Hodges and Dallimore, 2013). The modeled and simulated processes include baroclinic and barotropic responses, rotational effects, tidal forcing, wind stresses, surface thermal forcing, inflows, outflows and transport of salt, heat and passive scalars.

$$\frac{\partial u}{\partial t}+u\frac{\partial u}{\partial x}+v\frac{\partial u}{\partial y}+w\frac{\partial u}{\partial z}=-\alpha\frac{\partial p}{\partial x}+2\Omega v\sin\phi-2\Omega w\cos\phi+\alpha\frac{\partial \tau_x}{\partial z}-\alpha\frac{\partial \tau_b}{\partial x} \quad (1)$$

$$\frac{\partial v}{\partial t}+u\frac{\partial v}{\partial x}+v\frac{\partial v}{\partial y}+w\frac{\partial v}{\partial z}=-\alpha\frac{\partial p}{\partial x}-2\Omega u\sin\phi+\alpha\frac{\partial \tau_y}{\partial z}-\alpha\frac{\partial \tau_b}{\partial y} \quad (2)$$

$$\frac{\partial w}{\partial t}+u\frac{\partial w}{\partial x}+v\frac{\partial w}{\partial y}+w\frac{\partial w}{\partial z}=-\alpha\frac{\partial p}{\partial z}-g \quad (3)$$

where: $\alpha=\frac{1}{\rho_o}$. ρ_o is the water density. $\frac{\partial \tau_n}{\partial z}$ are the winds at 10m height, and n stands for the east and north wind components. P is water pressure. ϕ is a local latitude. To simulate a Macuse scenario, the Coriolis force was neglected in the simulation. Meanwhile, the water pressure, tidal currents water density, wind regime, water temperature and salinity were used in the model.

2.3. CAEDYM module for suspended sediments

The ELCOM model is the main physical driver that controls the coupled CAEDYM model. It provides spatially explicit, three-dimensional simulations of current and water temperature patterns based on processes including baroclinic and barotropic responses, rotational effects, tidal forcing, wind stress, surface thermal forcing, water inflows and outflows, passive scalars and sediment modules in all classes based on the Wentworth-1922a classification. The physical predictions generated, such as those for temperature, tidal elevation, salinity and tidal currents, establish a physical context for the use of the CAEDYM model to generate spatially explicit prediction processes of biological, chemical and geological parameters in different time scales (Zhao et al., 2009). The CAEDYM structure allows incorporating a submodule for suspended sediments, which generates spatial and explicit simulations of temporal variations. In this research submodule of the suspended sediment simulation is based on the calculation of suspended particles (inorganic particles) (Eq. (4)) as proposed by Hipsey and Hamilton's (2008).

$$\frac{\partial SS_s}{\partial t}=\frac{v_s}{\Delta Z}SS_s+\alpha S_s\frac{\tau-\tau_{cs}}{\tau_{ref}}\frac{SS_s-sed}{K_{ss_s}+SS_s-sed}\frac{1}{\Delta Z_{bot}}. \quad (4)$$

In which, SS_s is the concentration of inorganic suspended solids for group s (g m^{-3}); v_s is the settling velocity (m s^{-1}); Δz is the grid or layer thickness, αS_s is the resuspension rate parameter in g m^{-2} s^{-1}; τ is the shear stress (N m^{-2}), τ_{cs} is the critical shear stress for group s; τ_{ref} is a reference shear stress (1 N m^{-2}); K_{ss_s} controls the effect of sediment limitation on resuspension (g); and SS_s-sed is the sediment SS mass of group s (g). According to Hipsey and Hamilton (2008), a critical shear stress parameter τ_{cs} can be estimated from the dimensionless critical shield's parameter, which in turn is estimated from the dimensionless particle diameter D. Parameter D may be estimated as:

$$D=D_{s_s}\sqrt[3]{\frac{G-1}{\vartheta}g}. \quad (5)$$

Then G is the specific gravity of the re-suspended particles, g is gravitational acceleration (9.8 m s^{-2}), ϑ is the kinematic viscosity (10^{-6} m^2 s^{-1} at 20 °C) and D_{s_s} is the particle size. The critical shield parameter was calculated according to value of D:

$$D=\begin{cases}0.5\tan\alpha\Rightarrow D<0.3\\ 0.25D^{-0.6}\tan\alpha\Rightarrow 0.3<D<19\\ 0.013D^{0.4}\tan\alpha\Rightarrow 19<D<50\\ 0.06\tan\alpha\Rightarrow D>50.\end{cases} \quad (6)$$

In which α is the angle of repose of the sediment from 30°to 42°. The critical shear stress is then estimated from the equation,$\tau_{cs}=\tau\,(\gamma_s-\gamma_m)\,Ds$; $\gamma_s=\rho_s g$ is the specific sediment weight; and $\gamma_m=\rho_m=9800$ N m^{-3} is the specific weight of the water–sediment mixture. Based on Stoke's Law the settling velocity is calculated by

using the particle density, ρ_{s_s} and diameter D_{s_s}:

$$v_s = g\frac{\rho S_s - \rho_w(T,S)}{18\mu(T)}\left(D_{s_s}\right)^2 \quad (7)$$

where ρ_w is water density calculated dynamically as a function of temperature and salinity; and μ is the dynamic viscosity of water calculated internally as a function of temperature.

2.4. Model implementation

2.4.1. Pre-processing

The model configuration for the Macuse estuary was implemented according to the Hodges and Dallimore (2013) scheme (Fig. 2). The numerical code of the ELCOM was written in the Fortran-90 language. The diagram summarizes the key variables for the module execution, including pre-processing, model execution and visualization. The configuration of suspended sediment variables was based on the CAEDYM module under initial conditions and their preparation that consider the geochemical and biological variables. The data defined in ELCOM – CAEDYM were processed simultaneously for the production of Network Common Data Form (NetCDF) files in three types – vertical, horizontal curtain and mesh profiles. The post-processing phase corresponds to the results in NetCDF format that were converted and visualized through Fortran-structured commands and Matlab.

A map totaling 600 km^2 at a 1:10 000 scale (1998–99 at GCS-WGS-1984, Tete 36) was digitized with MIKE21 from a bathymetric chart obtained by *Instituto Nacional de Hidrografia e Navegação de Mozambique*—INAHINA. The bilinear interpolation technique was implemented with the model algorithm provided automatically by the Mike21. Although this technique is not more accurate than the triangular interpolation technique, the errors did not affect significantly the specific purpose of this study. Therefore, for the bathymetry accuracy we updated bathymetry points with the field measurements conducted with an echo-sounder Garmin 150. The final interpolated bathymetry was configured with a mesh grid of 20 m × 20 m (Fig. 4), with 230 *x*-rows and 190 *y*-columns and 10 vertical layers. The ELCOM geographic position was identified as −0.707107 north-*x* and +0.70711 north-*y*, which corresponds to 17.82°S and 37.07°E. The mesh grid was converted into an ELCOM—CAEDYM configuration within four open boundary conditions, including: 1-ocean boundary in *x*-row 230 and between *y*-column 80 and *y*-column 129 and at all layers; 2-runoff flow to the estuary in row 1 and between columns 112 and 120; 3-lateral runoff flow between rows 42 and 55 in the first column; and 4-lateral river flow between rows $X = 171$ and $Y = 176$ in *y*-column 61. In the two upstream boundaries (2 and 3), we applied the water discharge forces and sediment concentrations. In the downstream boundary 1 (ocean boundary), the tidal elevation from the Model-tpxo7 with a global resolution of 1/4° × 1/4° between January 2000 and December 2014 was implemented (www.coas.oregonstate.edu/research/po/research/tide/index.html). These included eleven tidal constituents: M2, S2, N2, K2, K1, O1, P1, Q1, MF, MM and M4, which began at 00:00, 01/01/2014 (17.76°S and 37.22°E). Their contributions are presented in Table 1.

2.4.2. Initial conditions

Initial conditions were implemented at the three boundaries (BC-1, BC-2, and BC-3) to execute the model, including water level, water temperature, water salinity, runoff and fine sand and silt concentrations (Table 2). At all of the boundaries, constant values of water salinity and water temperature were defined, and every volume of water in the computational domain was considered to be quiescent and vertically well mixed. A time interval of 120 s was defined for the simulation, for which 210 000 iterations were performed, and the output data were recorded hourly.

Table 1
Tidal constituents at water level boundary 1.

Constituent	Amplitude (m)	Phase (deg)
M2	1.1001	41.05
S2	0.6328	82.59
N2	0.1862	25.80
K2	0.1784	79.10
K1	0.0315	354.23
O1	0.0499	345.74
P1	0.0092	10.20
Q1	0.0135	321.14
MF	0.0121	2.57
MM	0.0058	355.49
M4	0.0085	334.63

Table 2
The initial conditions at the boundary interfaces. Where BC-1 represents the Macuse estuary entrance, BC-2 the right tributary and BC-3 the Namacurra River.

Parameter of initial condition	Model boundary		
	BC-1	BC-2	BC-3
Initial uniform water level (m)	2.6	1.0	1.0
Initial uniform temperature (°)	29	29	29.2
Initial uniform salinity (PSU)	29	29	27.5
Initial uniform sand concentration (mg l^{-1})	0	0	0
Initial uniform silt concentration (mg l^{-1})	0	0	0
Initial uniform water runoff (m^3 s^{-1})	0	300	500

2.4.3. Model execution

The model was configured to run a simulation of 14 months, which included the summer and winter seasons. This was due to significant variations in seasonal conditions that may have relevant impact on the runoff discharges, sediment supply, wind force and solar radiation. These factors may affect the water temperature, water salinity, biological activity and estuarine and ocean circulation.

Regarding the simulation applied to the Macuse estuary, a spin-up period of 5 days was implemented according to the model stability to guarantee the initial hydrodynamic conditions (Table 2). A time step of 60 s was adopted to ensure numerical stability with 555,000 time steps, with hourly saving of output data. The model was run for one month for spin-up verification and then performed a one-year run, which was completed after two weeks of simulation. The stabilization time was calculated according to the equation:

$$\sqrt{g'D}\frac{\Delta t}{\Delta x} < \sqrt{2}. \quad (8)$$

In which g' is equal to 100 (maximum parameter estimated for shallow water), $D = 15$ m (average depth of the estuary) and $\Delta x = 20$ m (corresponding to the dx size of the bathymetry). The model stability constant was estimated using the equation:

$$CFL = \frac{\Delta t U}{\Delta x}. \quad (9)$$

3. Results

3.1. Evaluating model results

To ensure the accuracy of the simulated tidal elevation within the model domain, the model was calibrated and validated using data obtained from a tidal gauge and CTD profilers fixed at station M3 (the port zone). In this case, the water levels were reproduced excellently, indicating the ability of the numerical model to describe the features of the tidal signal such as phase, amplitude, and ebb to flood tides, and the spring to neap variation of the tidal range. The results of this analysis indicated that the model reproduced well the tidal elevation of 4 m, tidal currents of 120 m s^{-1},

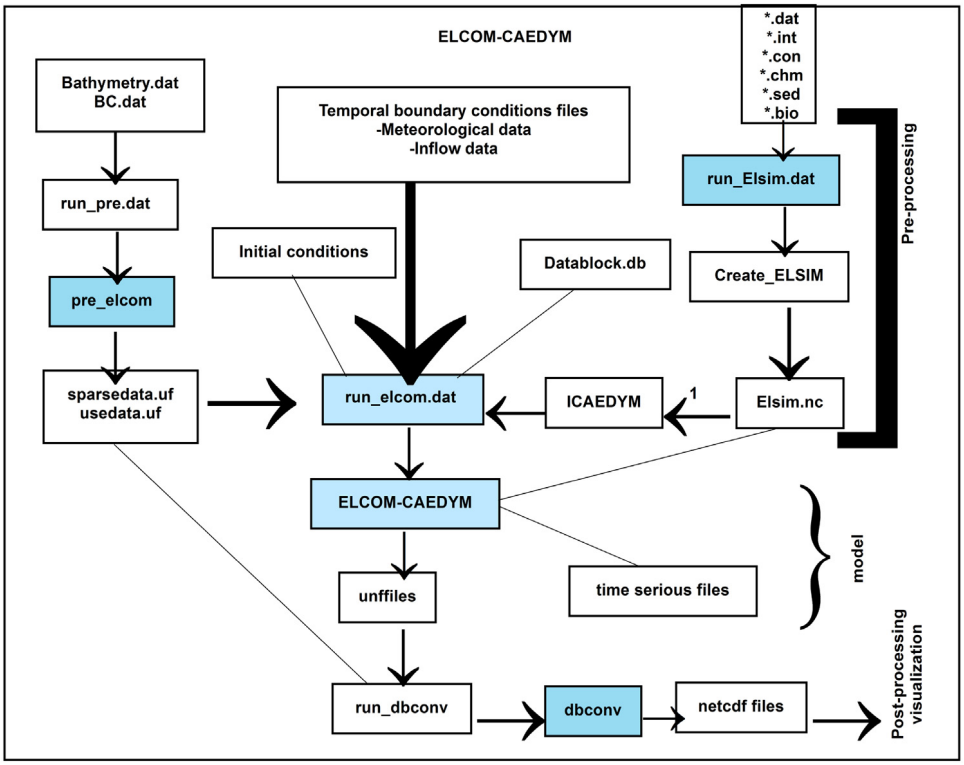

Fig. 2. Schematic diagram for ELCOM—CAEDYM module (Hodges and Dallimore, 2013).

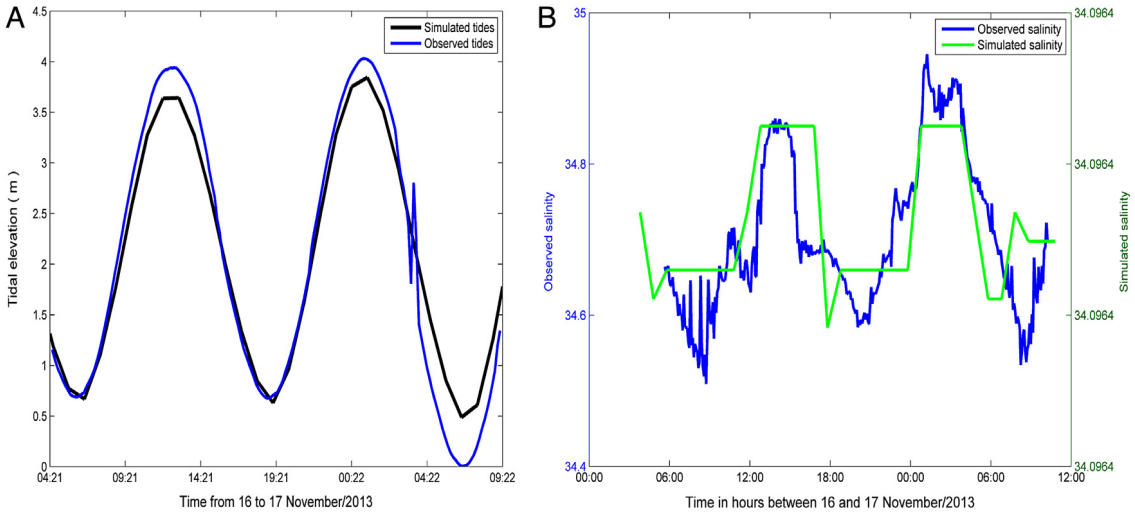

Fig. 3. A—Comparison between the observed and modeled tides. B—Comparison between the observed and simulated salinity.

and salinity variation between 34 and 35 (Fig. 3). These excellent matches between the observed and modeled data, confirm the accuracy of the model, capturing both the tidal amplitudes and the tidal phases in a significant correlation of $R^2 = 0.86$, whereas the correlation of observed and modeled salinity was estimated at $R^2 = 0.79$. These significant correlations indicate the accuracy of the model performance in the Macuse River estuary for both neap and spring tides for all conservative parameters.

For sediment verification, the comparison between the observed and simulated sediments was conducted at stations M1, M3 and M5 (Table 3, Fig. 4). Both observed and the modeled results matched well with $R^2 = 0.88$. Moreover, it is important to note that the 88% accuracy obtained indicates the robustness of the model performance for satisfactorily reproducing data outputs for suspended sediments.

Specific evaluations indicated that the tidal regime with a maximum height of 4 m had the role of generating the tidal currents (Fig. 5). These tidal currents with a maximum velocity of 120 cm s^{-1} reached their peak after the flood tides in both the spring and neap tides. It is important to notice that the estuary geometry defined the U-velocity as the main factor that controls the estuarine circulation with maximum tidal currents of 70 cm s^{-1} at station M3 (Fig. 6). The ebb and flood tidal currents had a strong correlation with the suspended sediments, which were estimated at $R^2 = 0.91$. This correlation is highly significant and reflected in the relative low suspended sediment concentrations of 110 mg l^{-1}

Table 3
Observed and simulated suspended sediments and their correlation on 16 and 17/11/2013 in Fig. 4.

Stations	Depths (m)	Obs. SS (mg l^{-1})	Simulated SS (mg l^{-1})
M5	1	111	120
M5	5	159	170
M5	10	240	250
M3	1	100	110
M3	5	168	160
M3	10	61	130
M1	3	301	250
M1	7	307	260
M1	12	212	170

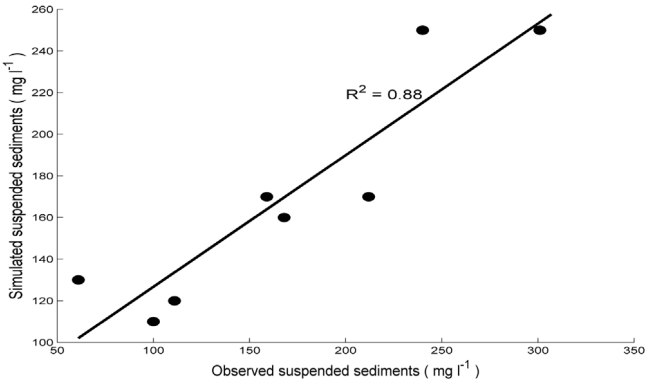

Fig. 4. Comparison between the observed and simulated suspended sediments.

during ebb tides, while flood tides were characterized by relatively high-suspended sediment concentrations of 160 mg l^{-1}.

3.2. Synoptic data

The 1:10 000 scale bathymetry interpolated with Mike21 demonstrated a configuration that indicated shallow depths in the entrance region and relatively deep depths along the river (Fig. 6). The EW river orientation combined with the geomorphology, permitted the U tidal currents flux to be stronger than the V-velocity component. According to the depths presented, site A demonstrated that it is narrower and deeper (14 m depth) than B which explains why it is favorable for the port construction. Despite the minimum depth of 2 m at the river entrance, the 4 m tidal regime allows water depths of 6 m at flood tides, which has set minimum vessel draft for navigation.

Particular analyses are focused on bed level variations beyond the vicinity of the Macuse River and the proposed areas (A and B) for the port construction. Special attention was given to the area of the tidal entrance, which is very important due to its effects on sediment transport by U-velocity (Fig. 10). Indeed, the U-velocity variation between −20 and 80 cm s^{-1} is responsible for bed level variations caused by hydraulic erosion. The erosion process is the primary factor in the channel deepening of the Namacurra River and sedimentation at its entrance. This sedimentation is very strong at the river entrance due to the weak U-velocity intensity, therefore, it begins to weaken along the channel to the Macuse River. The lower depths found at the entrance to the Macuse River give way to the primary tidal flow, eventually becoming a depositional area due to sediment supply from the rivers.

The bathymetry defined has different water fluxes according to the slope and geometry of the riverbed. Therefore, the water discharges are the second factor that contributes to the water's current flux and sediment transport combined with the sedimentation or erosion process. The maximum runoff discharges of 850 m^3 s^{-1} in March fed by average rains of 1000 mm $year^{-1}$ have a strong role in the supply and transport of sediment and the sedimentation that accumulates at the entrance of the Macuse River. This runoff is diluted by ocean water during the rainy season and leaves the Macuse River with two water types and in a quite turbulent state. Indeed, in situ observations of tidal free-surface elevation data indicated that high tidal and low tidal elevations drove the tidal currents and salinity distribution along the estuary.

A close association between the tidal elevation and tidal current was observed during the transition between the ebb and flood tides and vice-versa. There was a strong correspondence between salinity variation and daily tidal variation measured between 07:00:00 h and 09:17:00 h from 16 to 17 November/2014, with salinity found to be 35.9 at flood tides and 35.5 at low tides. The observed in situ temperature averaged 29 °C with no expressive changes in the period from 07:00:00 h to 09:17:00 h on 16 and

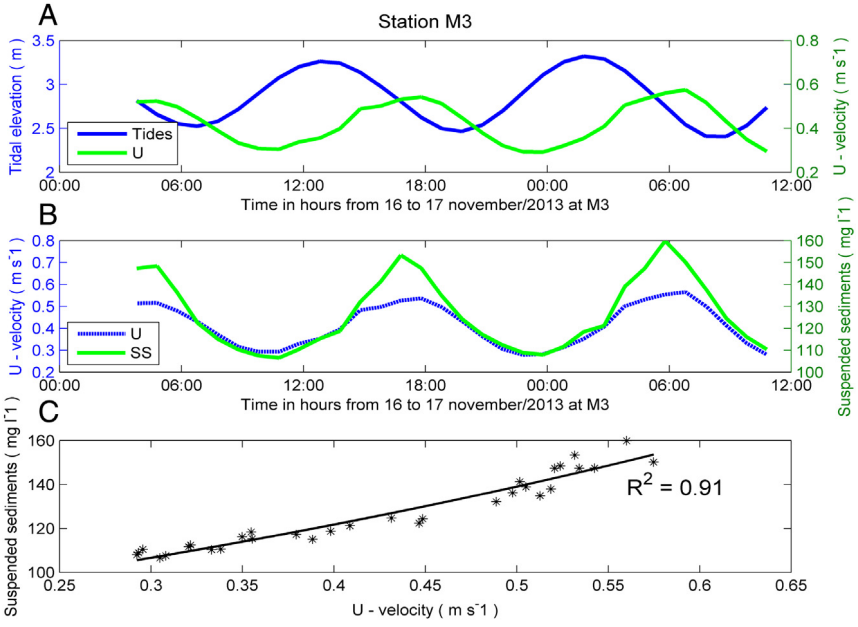

Fig. 5. A—Tidal elevation and U—velocity. B—Tidal elevation and suspended sediments. C—Correlation between U-velocity and simulated suspended sediments.

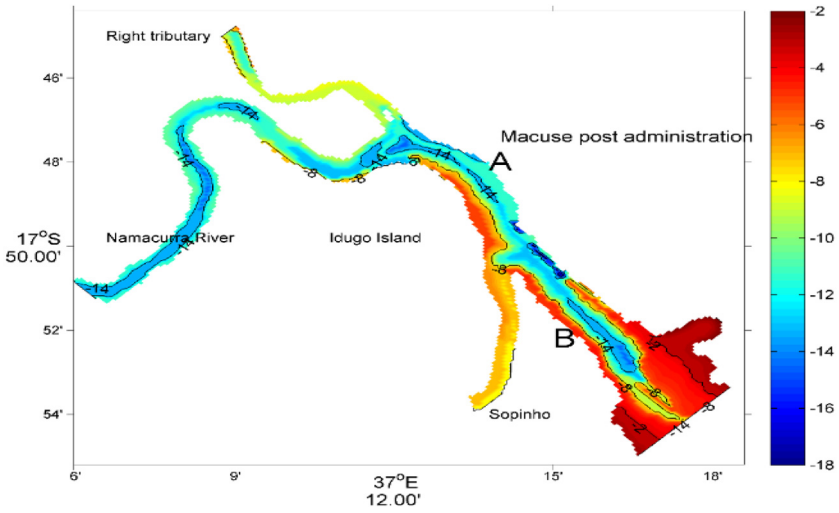

Fig. 6. Interpolated bathymetry using the bilinear method in the Mike21 model. A and B indicate the proposed sites for port construction.

17 November 2014. Field observations of turbidity concentration indicated relatively high values at the entrance of roughly 160 NTU and 120 NTU at the catchment. In the entrance zone, these concentrations indicated the strong tides influence, which are associated with bottom roughness, the water velocity and sediment size.

3.3. Model output data

The model outputs confirm the accuracy of the model for reproducing large-scale tidal patterns, tidal currents, salinity variation, temperature changes and suspended sediments. The tidal range of 4 m provides good documented information to explain the impact of the tides on the estuarine hydrodynamics studied. For example, at stations M1, M3 and M5, the water temperature and water salinity correlated well to explain the two possible water types in the T–S diagrams. These two water types include the ocean water with salinity changes between 34 and 36—A, while the freshwater and brackish water had salinity of less than 34—B (see Fig. 7a).

The average annual salinity at all stations (Fig. 7b), exhibited increasing salinity profiles with depth varying between 34.6 and 34.9 at M1, 32.4 and 34 at M3, and between 32.5 and 33.5 at M5. The changes presented make it quite evident that M1 had saltier water than M3 and M5, which presented fresh water discharges that diluted the ocean water to brackish water. Meanwhile, vertical temperature profiles with depth decreased from the surface to the bottom changing at M1 between 23.20 °C and 23.4 °C, at M3 between 20.8 °C and 21.3 °C and at M5 between 21.6 °C and 22.3 °C.

Based on the proposed Eq. (7), we identified a silt-settling velocity of 0.10 cm s^{-1}, and a fine-sand settling velocity of about 10 cm s^{-1}or less. These velocities explain why the fine sand was usually transported by dragging mechanics on the riverbed while the silt remained in suspension. Indeed, the Macuse geomorphology indicated that U-velocity is the main factor that drives the hydrodynamics of the Macuse estuary. The velocities presented in Fig. 8 indicate a maximum of 20 cm s^{-1} in the rainy season, which is higher than the settling velocity for both fine sand and silt. The maximum velocity was reached during the spring tides in the ebb period with a maximum of 120 cm s^{-1}. Minimum velocity of 0 cm $s^{-1}$was detected during the transition tides between ebb and flood periods. Figs. 8a and 8b, makes it quite evident that zero velocities are found at the bottom layers suggesting proper conditions for fine sand and silt settling.

In both rainy and dry seasons, it is evident that the mixing energy was driven by water current patterns. In response, strong mixing occurred when the water speed was over 10 cm s^{-1}, and possible stratification when water speed was less than 10 cm s^{-1} for fine sand and 0.10 cm s^{-1} for silt. Indeed, for example, the fine sand was usually transported on the bottom layers by dragging, while the silt fluxes were distributed at all water layers with concentrations ranging between 180 and 260 mg l^{-1}. During the flood tide, due to the lower river intake and increased tidal elevation, the suspended sediment (SS) concentrations reached between 180 and 300 mg l^{-1}. Smaller SS concentrations were observed in the dry season, influenced by the modulation of the local tide, which ranged between 180 and 200 mg l^{-1}. During ebb tides, the highest SS concentrations occurred near the entrance of the estuary and was influenced by the resuspension process.

The rising tide increased the SS concentration from the inner estuary to the harbor zone. In the transition between stations M1 and M5, the U-velocities drop expressively because of the converging movements between the river discharge and tidal propagation (Figs. 8a, 8b). It is evident that the main source of silt and fine sand is the Namacurra River. The water discharge from the Namacurra combined with tidal currents drives silt and fine sand downstream in the estuary. In addition, this combination is responsible for the advective transport of suspended matter, water salinity, and water temperature in the Macuse estuary (Figs.8a, 8b).

It was observed that in the rainy season, the transport of salt was predominantly associated with runoff from the Namacurra River and the right tributary, forcing the salt water to the entrance and demonstrating the strong fluvial influence during the rainy season. In the dry season, the runoff was low and the salt water was transported upstream in the estuary to the catchment zone. The downstream transport during the ebb tides the water salinity had values close to 35. Salt accumulation at the catchment may result between May and December, when was observed a negative water balance and salinization oriented upstream (from the ocean to the Namacurra River). The transport of salt associated with the river discharge was more strongly influenced by tides at all the stations in the dry season due to the reduced storage of freshwater during the tidal change. The simulated temperature data indicates that the warmer water came from the river, while the colder and saltier water moved from the ocean to the river. The combination of temperature and salinity generated water densities (sigma-t) between 20 and 24 kg m^{-3}, which suggest a mixture of more ocean water than runoff. The mixture was expressive due to the ocean water retention-time of 5 days.

In both the rainy and dry seasons, the wind energy at the surface was about 30 $\times$ 10^{-6} J and reached bottom layers at about 3

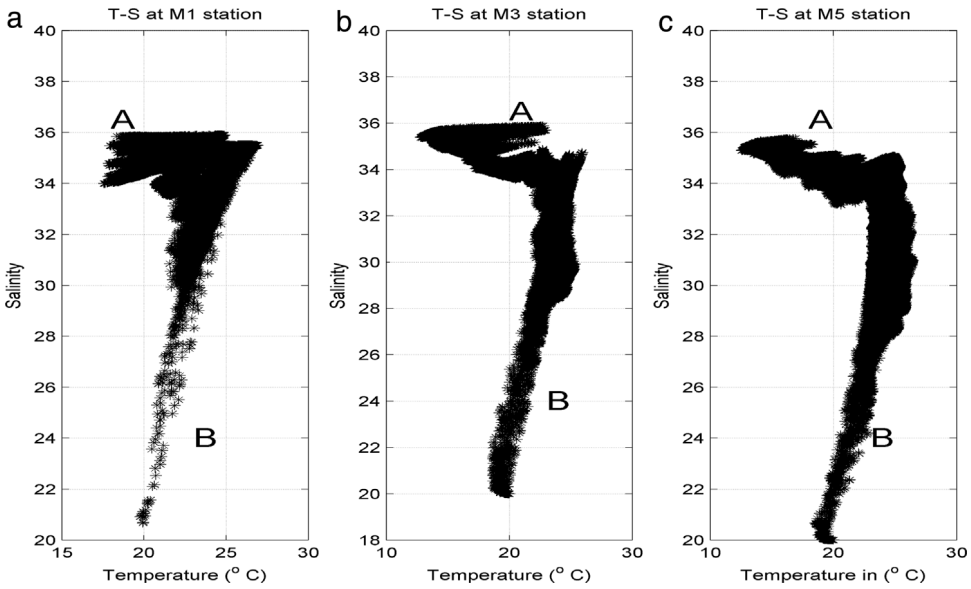

Fig. 7a. The annual T–S diagrams (a, b and c) and the relation between salinity and suspended sediments (d, e, f) at the defined stations M1, M2 and M3. B—Indicates the brackish water and runoff discharges. A—Indicates the ocean water type.

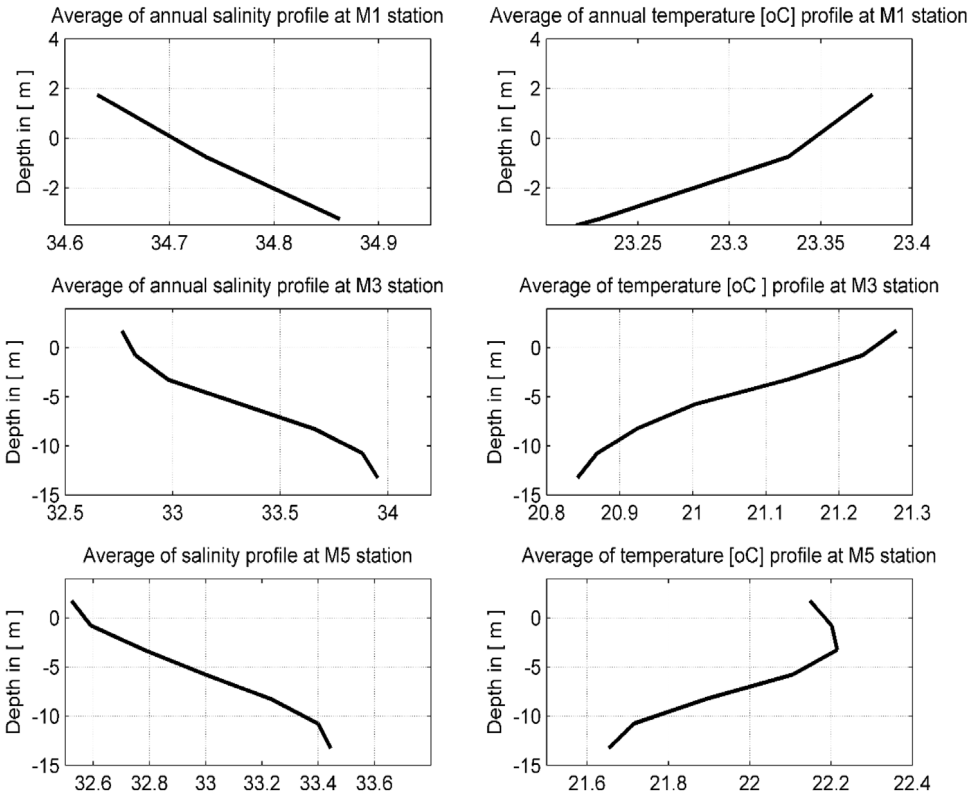

Fig. 7b. Average annual salinity and temperature profiles at stations M1, M2 and M3.

m, which contributed to water mixing and suspended sediment transport. The shear energy at the bottom was about 10^{-4} J in the rainy and dry seasons, while the shear energy along the water column was about 200×10^{-6} J in both the rainy and dry seasons. These parameters had a strong role in the water mixing in both seasons due to the ebb and flood tides. The dissipation energy was about 1 J with high values observed at the entrance.

The water salinity distribution reflects the combination of all the transport processes, including density changes, stratification and mixing. These processes in turn control density circulation and modify the water-column mixing. Turbulent mixing plays a critical role in determining the stratification and residual circulation of Macuse estuary. Meanwhile, the suspended silt and fine sand concentrations are results of the mixing process and hydrodynamics, in which the spatial and time distribution is controlled by persistent tidal changes. In this case, the maximum concentration predicted was about 300 mg l^{-1} with high concentrations during spring tides and concentrations lower than 100 mg l^{-1} during ebb tides in neap tides (Figs. 9a and 9b). The results indicated strong currents where the bathymetry presented a steep topographic

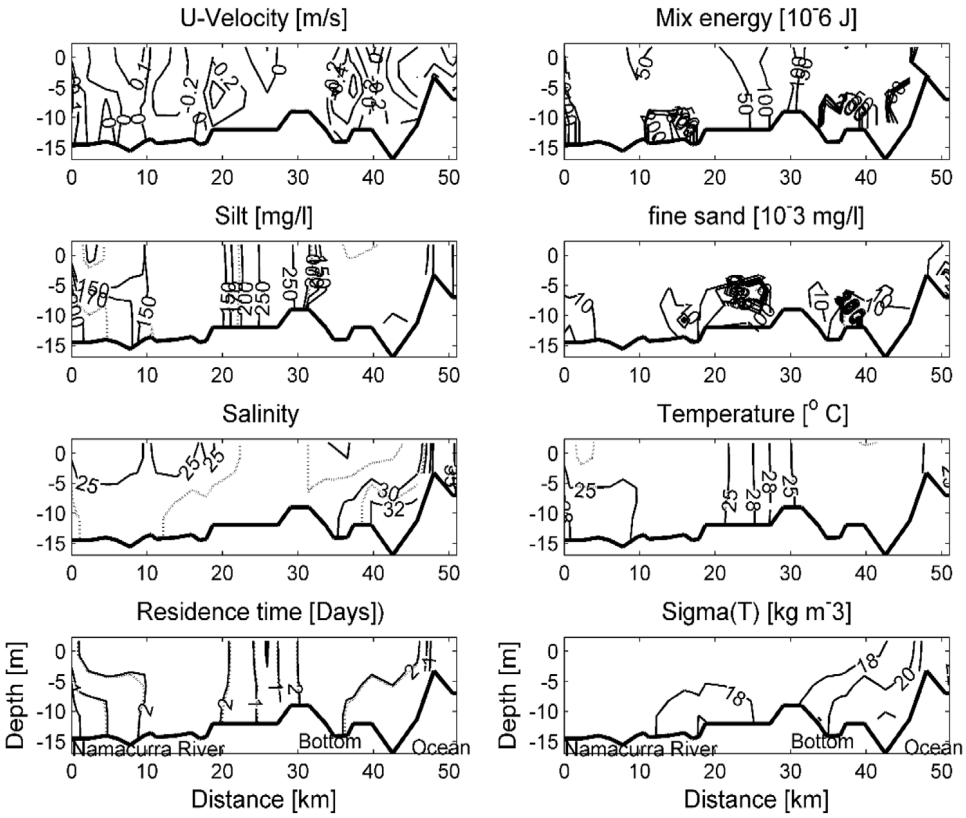

Fig. 8a. Typical results of simulated data during the rainy season in 2014.

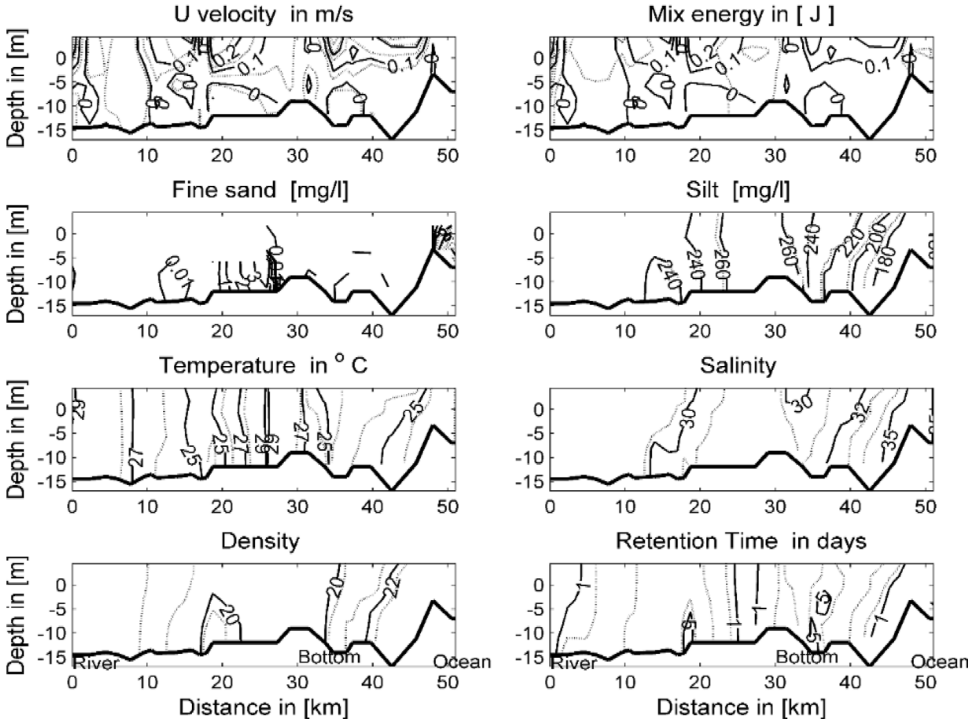

Fig. 8b. Typical results of simulated data during the dry season in 2014.

slope that usually projects suspended sediments downward or leftward of site A (see Fig. 4).

The 4 m high tides were responsible for the absolute speed changes between 0 and 120 cm s^{-1} (Figs. 9a and 9b). The periodic speed changes were strong during spring tides and relatively weak during neap tides. The role of these speeds ware reflected in the suspended sediment concentration in the water column during the rainy and dry seasons.

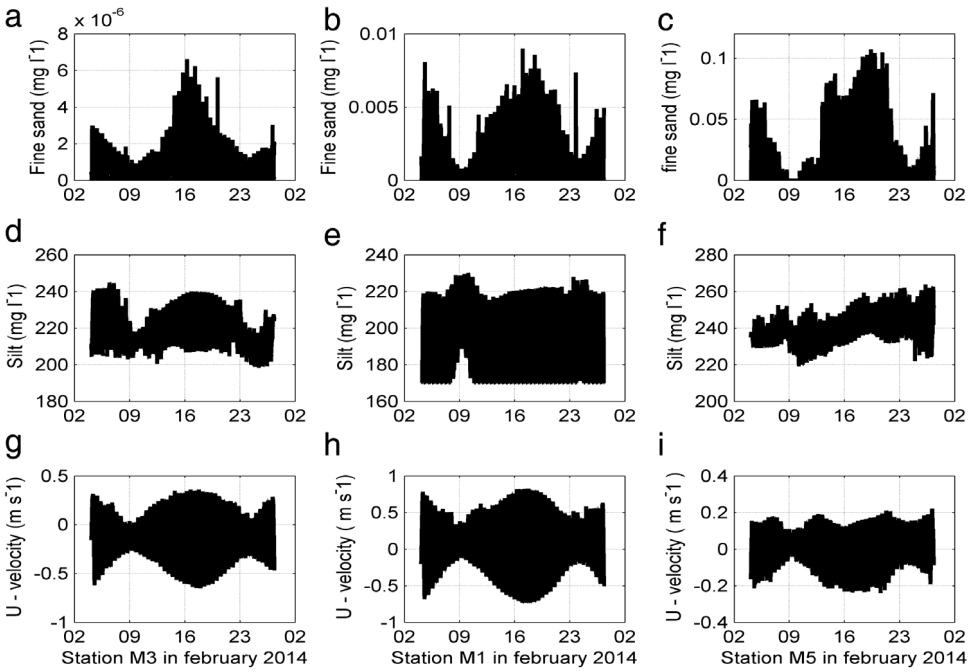

Fig. 9a. Short time serious of fine sand (a, b, c), silt (d, e, f) and U-velocity (g, h, i), in the rainy season.

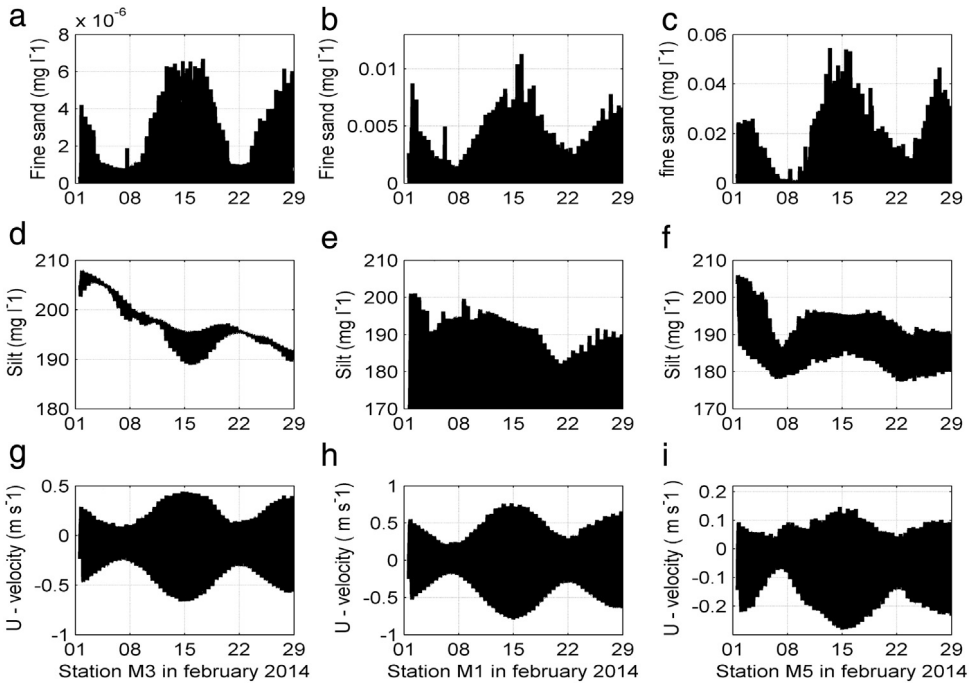

Fig. 9b. Short time serious of fine sand (a, b, c), silt (d, e, f) and U-velocity (g, h, i), in the dry season.

In the transition period from the neap to spring tides, the concentration of suspended sediments changed from a 100 to 270 mg l^{-1}. The separated investigation of the rainy and dry seasons facilitated a more thorough analysis of suspended particles, which allowed us to identify and quantify the variation of several physical parameters correlated to sediment transport and their characteristics. In this case, for the sake of simplicity, results from the rainy season indicated a strong correlation between the suspended sediments and tidal oscillation. This was observed in the high concentration of both fine sand and silt during the spring and flood-tides (Figs. 9a and 9b). The fine sand flux was not observed expressively in the simulation because of the high weight and relatively high density. Despite the relatively unexpressive concentration of the fine sand in the rainy and dry seasons, low concentrations were observed with a maximum of 0.15 mg l^{-1}. During the dry season, there were strong changes in the suspended sediments with relatively lower concentrations than that of the rainy season. The changes were caused with no significant discharges from the main boundary rivers and were immediately reflected in the low concentrations of suspended sediments.

Pronounced changes in concentration between the rainy (in February) and dry season (in June) were observed in our analysis (Figs. 9a, 9b). At station M3, silt concentrations were relatively low and unexpressed fine sand concentrations were observed in the two seasons. The results reflect a strong relationship between the variation in the tidal currents and direct changes in the suspended sediment concentrations. While the runoff discharges are observed seasonally with relatively large concentrations in the rainy season between January and May and relatively low concentrations during the dry season between July and December (Figs.9a, 9b). More generally, these results illustrate the intimate relationship between the tidal flow and sediment transport patterns of the two groups (silt and fine sand). In response, may have a role in the morphodynamics that may be expected from any alteration of the Macuse estuary bathymetry.

Specific results in February illustrated that the estuary geomorphology and topography configuration may control the U-velocity, which governs the suspended sediment in the Macuse estuary. This process was confirmed at station M3 where the maximum concentration of sand was 6×10^{-6} mg l^{-1}, while 8×10^{-3} mg l^{-1} was observed at station M1 and 0.10 mg l^{-1} at station M1. These concentrations indicate each station's dependence on the main sources of sediment and tidal energy. Silt concentration values between 220 and 261 mg l^{-1} were observed at station M5 with the U-velocity ranging between −21 and 20 cm s^{-1}. The concentration was about 200 and 240 mg l^{-1} when the U-velocity was between −50 and 50 cm s^{-1} at M3. Moreover, at the station M1 with U-velocity between −50 and 50 cm s^{-1} was registered silt concentration between 170 and- 230 mg l^{-1}. Both results for silt and fine sand presented differences between February and June and an intimate relation with the driving U-velocity and runoff discharges.

Vertical profiles of suspended fine sand at stations M1, M3 and M5 increased with depth from the surface to the bottom with a maximum of 0.015 mg l^{-1}(Fig. 10). This suggests the dragging transport process on the riverbed by tidal currents combined with the river slope that increases the gravity water flux. Contradictory to the fine sand, the silt decreased with depth from the surface to the bottom at the M1, M3 and M5 stations. At station M1, the annual average silt concentration changed between 179 and 118 mg l^{-1}. At station M3 the silt changed between 204 and 214 mg l^{-1}. At M5 the annual average silt concentration changed between 208 and 212 mg l^{-1}. These annual profiles suggest that silt and fine sand sources are the Namacurra River and right tributary that decrease expressively their concentrations towards the river entrance.

4. Results discussion

The field and modeled data outputs agreed that there is a strong relationship between tidal oscillation and tidal currents, as well as with suspended sediments. Tidal currents, gravity flow, and river discharge were previous identified by Dias et al. (2016) as the three forces responsible for the advective transport of salt in estuarine systems. The results obtained in this research indicated that might cause additionally the advective transport of suspended sediments (silt and fine sand).

The tidal range of 4 m in height proved that the Macuse estuary is dominated by tidal currents with sufficient tidal prism that permits the river entrance maintain against longshore and cross-shore wave-driven littoral sediment transport. Despite the mesotidal regime found in Macuse estuary, the results agree with those of Cooper (2001) in microtidal estuaries of Republic of South Africa. Furthermore, the magnitude of the tide and the runoff discharges determined the concentration of suspended sediments closer to the catchment and entrance. Thus, the higher the magnitude of the tides or runoff discharges, the higher the suspended sediments concentration during the dry or rainy seasons. These results are in good agreement with those of Dias et al. (2016), Kitheka et al. (2005) and D'Aquino (2010) in similar systems.

The unidirectional flows of U-velocity indicated that in the dry season, marine waters have a greater influence on the estuary system, which results in flood tides that are higher than ebb tides at stations M1, M3 and M5. Dias et al. (2016), Stanev et al. (2007) and Dias et al. (2013b) recently experienced same related results in similar environments. The U-velocity results suggest that the Macuse estuary is well mixed and the ocean water is transported upstream predominantly via tidal propagation. The stationary U-velocity pattern in the estuary revealed the fluvial influence on the estuarine system, which diminished the water salinity to 30 during the rainy season between January and March. Dias et al. (2013b) state that positive values for U-velocity during the rainy season may transport freshwater downstream. This process was found at the Macuse estuary where the freshwater was exported by a unidirectional U-velocity with a maximum of 80 cm s^{-1}. The transport of runoff from the Namacurra River in the rainy season generated positive current velocities (downstream from the estuary) during both the flood and ebb tides. However, in the dry season, the flood velocities indicated the entrance of ocean water with salinity of about 35 (Fig. 8).

Field results revealed expressive suspended sediment concentrations with a maximum of 307 mg l^{-1}, while the predicted suspended sediment concentrations indicated a maximum of about 300 mg l^{-1}. In fact, the concentration of suspended sediments changed cyclically as a function of tidal variation and seasonal runoff discharge volume. These concentrations revealed a vertical light attenuation caused by the concentration of suspended sediments of 300 mg l^{-1} and runoff discharges from the main boundaries. On the other hand, the turbidity between 120 NTU and 160 NTU revealed the attenuated light penetration in the water column, which corroborates the explanation given by Bowers et al. (2004), Mills et al. (2002), Painting et al. (2007), Devlin et al. (2008) and Corbett (2010), who found that opaque particles in the water block the light penetration.

Seasonal suspended sediments results indicated relatively higher suspended sediment concentrations in the rainy season than in the dry season. The tidal modulation combined with river discharge influenced the highest suspended concentrations during the rainy season. While the low suspended concentrations during the dry season were influenced by the tidal modulation. These results are similar to those reported for other similar estuaries (Kitheka et al., 2005; Schettini, 2003; Cooper, 2001). The deposition and resuspension was related to cyclic changes in tidal currents (Fig. 8a), which corroborate conclusions of Brockmann and Dippner (1987), Boon and Duineveld (1996), Stanev et al. (2007), Schettini (2003), Shi and Kirby (2003) and Chen et al. (2005) in similar environmental conditions. The suspended particulate matter and resuspension matter from the bottom was usually caused by tidal changes, which agrees with the findings of Tian et al. (2009) in a similar environment. Tidal currents are the main controlling factor that governs the water circulation and re-suspended sediments in the Macuse estuary. Because of the tidal currents, the fine sand settled quickly at the main boundaries because of the weight, viscosity, gravity, density and bottom roughness. In contrast, silt was transported significant distances in the water column. These results agreed with those of Hurzeler et al. (1995) in a similar study, who concluded that the suspended sediment deposition changes the buoyancy of the inlet flow density and changes the background flow to the surface over a relatively short distance. In this case, the tidal dynamics provide strong evidence of their role in the transport of suspended sediments during the spring and neap tides of about 300 mg l^{-1}.

Various studies around the world (Dias et al., 2016; Cooper, 2001; Brockmann and Dippner, 1987; Kitheka et al., 2005; Tian et

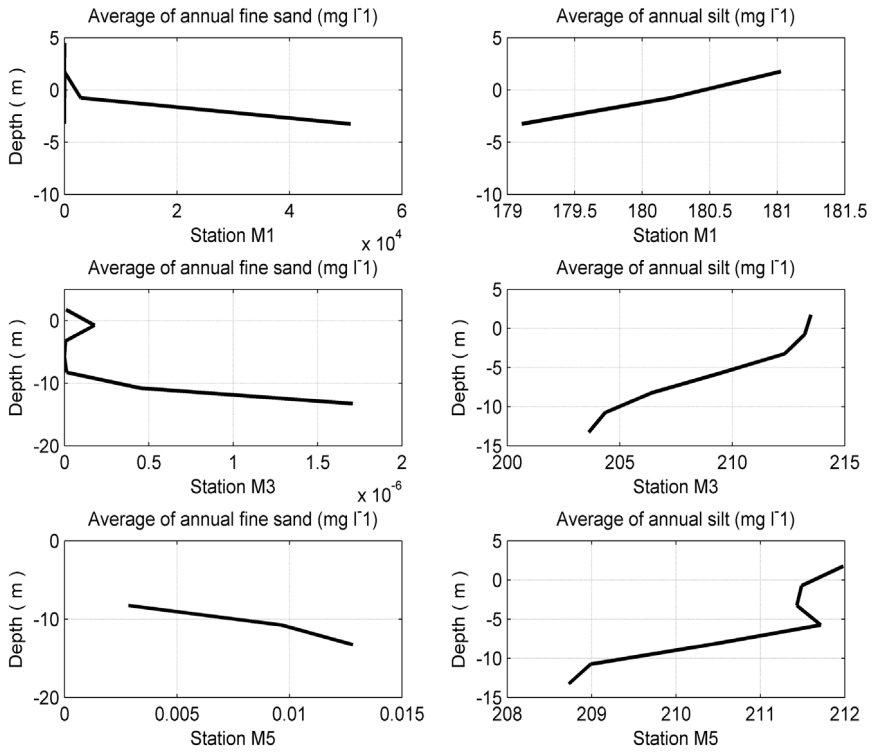

Fig. 10. Annual vertical profiles of fine sand and silt at M1, M3 and M5.

al., 2009; Boon and Duineveld, 1996; Stanev et al., 2007; Shi and Kirby, 2003; Chen et al., 2015) agree that sediment transport in estuaries is governed by tidal dynamics and tidal asymmetry, plus their relationship with the runoff discharges and geomorphology. However, it is worth noting that other factors may control sediment transport such as bed roughness, margin friction, sediment density and fluid viscosity. This may raise questions about the scale of uncertainty from the modeling of complex natural environments such as the Macuse estuary. Indeed, there are many factors to be considered, including environmental patterns, relative sea-level rise/fall, sediment supply and river discharges in different scales. These factors may be responsible for sediment transport and any modeling process should question the quantities of output data. Despite these issues, general numerical modeling approaches in estuarine systems tend to support analysis, contributing to the understanding of existing processes (*e.g.* Macuse estuary system).

Recent analyses have allowed researchers to increase the accuracy of models used in the planning of estuary development and of changes caused by different development phases. For example, the data results obtained in this study show that the two sites proposed for harbor construction by the Mozambique government have stronger potentialities at site A than B. The suitable oceanographic potential found at site A is supported by the relative insignificant suspended sediment deposition and the 25 m depth of the site. These conclusions sustain the hypothesis that no dredging would be needed at site A over a long time scale, while site B would be strongly affected by the weak current speed of 20 cm s^{-1} and suspended sediment deposition index. These factors are aggravated by the 4 m depth, which is not suitable for ship navigation. The benefits of understanding the sediment transport and estuarine morphodynamics may extend beyond their importance to the hydrodynamics and bathymetry at the Macuse estuary to policy and political decisions about the estuary's sustainability and local coastal management.

5. Conclusions

1—The 4 m high tidal regime generated tidal currents of 120 cm s^{-1} during the transition period between the ebb and flood tides and vice-versa. The critical silt settling velocity was 0.10 cm s^{-1}, while the fine sand velocity settling speed was found to be 10 cm s^{-1}, suggesting that the suspended sediments were maintained in the water column when the tidal currents were greater than critical velocities.

2—Two water types were detected in both seasons, including water type A (ocean water) with salinity greater than 34 during the dry season and type B (brackish water) with salinity less than 30. Moreover, the wind mixing energy combined with the bottom and shear stress energy were controlling factors in the mixing of the estuary waters in both the rainy and dry seasons.

3—The field results indicated maximum suspended sediment concentrations of 310 mg l^{-1}, which confirmed the model's prediction of 300 mg l^{-1}, in which the comparison indicated a correction of $R^2 = 0.88$. During the rainy season, the suspended sediments had a greater concentration with a maximum of 300 mg l^{-1}, while in the dry season it was about 200 mg l^{-1}. The variation in tidal currents had a lead role in the transportation of suspended sediments during the rainy and dry seasons.

4—The comparison between the observed and simulated data demonstrated the accuracy of the ELCOM-CAEDYM model for predicting the role of the tides and river discharges in the dynamics of suspended sediments in the Macuse estuary, and that it may be applied to studies of other estuaries. The efficacy of the model in understanding the sediment transport mechanism will help making political decisions about the estuary's sustainability and local coastal management.

Acknowledgments

We are grateful to the MCT—**Mozambique** for financing this project and to the **Eduardo Mondlane University** for the lab analyses and the availability of the multi-sensor instruments for the

field-data collection. We are grateful to the **Lwandle Company of South Africa** for the second phase of fieldwork in November 2014. Finally, we would like to thank **Dr. Kate Munnik** for her special attention to the data and her contributions. Moreover, we would like to thank **Stella Vaz** (Student at PPGI—Federal University of Rio de Janeiro in Brazil) for English grammar corrections.

References

Armitage, S.J., Botha, G.A., Duller, G.A.T., Wintle, A.G., Rebêlo, L.P., Momad, F.J., 2006. The formation and evolution of the barrier islands of Inhaca and Bazaruto, Mozambique. Geomorphology 82, 295–308.

Biggs, R.B., 1970. Sources and distributions of suspended sediments in Northern Chesapeake Bay. Mar. Geol. 9, 87–201.

Boon, A., Duineveld, G., 1996. Phytopigments and fatty acids as molecular markers for the quality of near-bottom particulate organic matter in the North Sea. J. Sea Res. 35 (4), 279–291.

Bowers, D., Evans, D., Thomas, D., Ellis, K., Williams, P., 2004. Interpreting the colour of an estuary. Estuar. Coast. Shelf Sci. 59, 13–20.

Brockmann, C., Dippner, J., 1987. Tidal correction of hydrographic measurements. Ocean Dyn. 40 (6), 241–260.

Chen, W., Liu, W., Hsu, M., Hwang, C., 2015. Modeling investigation of suspended sediment transport in a tidal estuary using a three-dimensional model. Taiwan. Appl. Math. Model. 39, 2570–2586. http://dx.doi.org/10.1016/j.apm.2014.11.006.

Chen, S.L., Zhang, G., Yang, S.L., Shi, J.Z., 2005. Temporal variations of fine suspended sediment concentration in the Changjiang River estuary and adjacent coastal waters, China. J. Hydrol. 331, 137–145. http://dx.doi.org/10.1016/j.jhydrol.2006.05.013.

Chevane, C.M., Penven, P., Nehama, F.P.J., Reason, C.J.C., 2016. Modeling the tides and their impacts on the vertical stratification over the Sofala Bank, Mozambique. Afr. J. Mar. Sci. (ISSN: 1814-232X) 1814–2338. http://dx.doi.org/10.2989/1814232X.2016.1236039. (Print).

Cooper, J.A.G., 2001. Geomorphological variability among microtidal estuaries from the wave-dominated South African coast. Geomorphology 40, 99–122 PII: S0169-555XŽ01.00039-3.

Corbett, D.R., 2010. Resuspension and estuarine nutrient cycling: insights from the Neuse River Estuary. Department of Geological Sciences, Institute for Coastal Science and Policy, East Carolina University, Greenville, North Carolina, USA. Published in Biogeosciences. Vol. 7, pp. 3289–3300. http://doi.org/10.5194/bg-7-3289-2010.

D'Aquino, C.A., 2010. Processos de transporte e retenção de sedimentos finos em estuários dominados por rios. Tese de Doutorado. UFRGS. Porto Alegre. Brasil.

Day, J.W., Pont, D., Hensel, P.F., Ibanez, C., 1995. Impacts of sea-level rise on deltas in the Gulf of Mexico and the Mediterranean: the importance of pulsing events to sustainability. Estuaries 18, 636–647.

Devlin, M.J., Barry, J., Mills, D.K., Gowenc, R.J., Foden, J., Sivyerb, D., Tett, P., 2008. Relationships between suspended particulate material, light attenuation and Secchi depth in UK marine waters. Estuar. Coast. Shelf Sci. 79, 429–439. http://dx.doi.org/10.1016/j.ecss.2008.04.024.

Dias, F.J.S., Castro, B.M., Lacerda, L.D., Miranda, L.B., Marins, R.V., 2016. Physical characteristics and discharges of suspended particulate matter at the continent-ocean interface in an estuary located in a semiarid region in northeastern Brazil. Estuar. Coast. Shelf Sci. 180, 258–274. http://dx.doi.org/10.1016/j.ecss.2016.08.006.

Dias, F.J.S., Marins, R.V., Maia, L.P., 2013b. Impact of drainage basin changes on suspended matter and particulate copper and zinc discharges to the ocean from the Jaguaribe River in the semiarid NE Brazilian coast. J. Coast. Res. 290, 1137–1145.

Fain, A.M.V., Jay, D.A., Wilson, D.J., Orton, P.M., Baptista, A.M., 2001. Seasonal and tidal monthly patterns of particulate matter dynamics in the Columbia River estuary. Estuaries 24 (5), 770–786.

Gelfenbaum, G., 1983. Suspended-sediment response to semidiurnal and fortnightly tidal variations in a mesotidal estuary: Columbia River, USA. Mar. Geol. 52, 39–57.

Grabemann, I., Krause, G., 2001. On different time scales of suspended matter dynamics in the Weser Estuary. Estuaries 24, 688–698.

Halo, I., Penven, P. Backeberg.B., Ansorge, I., Reason, C., Ullgren, J., 2014. Eddy properties in the Mozambique Channel: A comparison between observations and two numerical ocean circulation models. Deep Sea Res. Part II. http://dx.doi.org/10.1016/j.dsr2.2013.10.015. (in press).

Hanson, S., Nicholls, R., Ranger, N., Hallegatte, S., Corfee-Morlot, J., Herweijer, C., Chateau, J., 2011. A global ranking of port cities with high exposure to climate extremes. Clim. Change 104, 89–111.

Hipsey, M.R., Hamilton, D.P., 2008. Computational Aquatic Ecosystem Dynamics Model: CAEDYM v3. Centre for Water Research University of Western Australia.

Hodges, B., Dallimore, C., 2007. Estuary, Lake and Coastal Ocean Model: ELCOM v2.2. Science manual Centre for Water Research, University of Western Australia, p. 62 May 23.

Hodges, B., Dallimore, C., 2013. Estuary, Lake and Coastal Ocean Model: ELCOM v2.2. Science manual Centre for Water Research, University of Western Australia, p. 62 May 23.

Hodges, B.R., Imberger, J., Angelo Saggio, A., Winters, K.B., 2000. Modeling basin-scale internal waves in a stratified lake. Limnol. Oceanogr. 45 (7), 1603–1620.

Hurzeler, B.E., Ivey, G.N., Imberger, J., 1995. Spreading model for a turbidity current with reversing buoyancy from a constant-volume release. Mar. Freshw. Res. 46, 393–408.

Kitheka, J.U., Obiero, M., Nthenge, P., 2005. River discharge, sediment transport and exchange in the Tana Estuary, Kenya. Estuar. Coast. Shelf Sci. 63, 455–468. http://dx.doi.org/10.1016/j.ecss.2004.11.011.

Langa, J.V.Q., 2007. Problemas na zona costeira de Moçambique com ênfase para a costa de Maputo. Universidade Eduardo Mondlane, MoÇAmbique. Rev. Gestão Costeira Integrada 7 (1), 33–44.

Liu, X., 2014. Sediment dynamics off the east African continental margin during the last deglaciation and Holocene: Constrained by changes in climate and sea level. Bremen University. Dissertation.

Lutjeharms, J.R.E, van Ballegooyen, R.C., 1988. Anomalous upstream retroflection in the Agulhas Current. Science; Washington Vol. 240, no. 4860 (Jun 24, 1988), p. 1770.

Maskell, J., Horsburgh, K., Lewis, M., Bates, P., 2013. Investigating river-surge interaction in idealised estuaries. J. Coast. Res. 30, 248–259.

Miguel, L.L.A.J., 2013. Estudo da circulação hidrodinâmica e transporte de sedimentos no estuário de Macuse: Contribuição para a navegação e construção de um porto, Província da Zambézia - Universidade Eduardo Mondlane, Moçambique. 74pp.

Mills, D.K., Rutgers, M., Laane, R.W.P.M., Rees, J.M., 2002. Continuous measurement of suspended matter. Sea Technol. 43 (10), 5.

Moore, A.E., Cotterill, F.P.D., Main, M.P.L., Williams, H.B., 2008. The Zambezi river. In: Gupta, . (Ed.), Large Rivers: Geomorphology and Management.

National Institute of Hydrography and Navigation of Mozambique –INAHINA, 2013. Tabela de marés de 2013.

Nehama, F.P.J., 2012. Modelling the Zambezi River plume using the Regional Oceanic Modelling System. Thesis presented for the Degree of Doctor of Philosophy. Oceanography Department, Faculty of Science, University of Cape Town, South Africa. 177pp.

Nicholls, R.J., Hoozemans, F.M.J., March, M., 1999. Increasing flood risk and wetland losses due to global sea-level rise: regional and global analyses. Glob. Environ. Change Hum. Policy Dimens. 9, 69–87.

Nicholls, R.J., Marinova, N., Lowe, J.A., Brown, S., Vellinga, P., Gusmão, D.de., Hinkel, J., 2011. Sea-level rise and its possible impacts given a beyond 4 degrees world in the twenty-first century. Philos. Trans. R. Soc. A 369, 161–181.

Painting, S.J., Devlin, M.J., Malcolm, S.J., Mills, C., Mills, D.K., Parker, E.R., Tett, P., Wither, A., Burt, J., Jones, R., Winpenny, K., 2007. Assessing the impact of nutrient enrichment in estuaries: susceptibility to eutrophication. Mar. Pollut. Bull. 55, 74–90. http://dx.doi.org/10.1016/j.marpolbul.2006.08.020.

Patchineelam, S.M., Kjerfve, B., 2004. Suspended sediment variability on seasonal and tidal time scales in the Winyah Bayestuary, South Carolina, USA. Estuar. Coast. Shelf Sci. 59, 307–318.

Quinn, N.D., Lewis, M., Wadey, M., Haigh, I., 2014. Assessing the variability in extreme storm-tide time-series for coastal flood risk assessment. J. Geophys. Res. 119, 4983–4998.

Ramsay, P.J., 1995. 9000 years of sea-level change along the southern African coastline. Quat. Int. 31, 71–75.

Schettini, A.C.A., 2003. Estudo do regime de correntes e material particulado em suspensão ao largo do estuário do rio Itajaí-açu. Brasil. II Congresso sobre Planejamento e Gestão das Zonas Costeiras dos Países de Expressão Portuguesa.

Shi, Z., Kirby, R., 2003. Observations of fine suspended sediment processes in the turbidity maximum at the North Passage of the Changjiang Estuary, China. J. Coast. Res. 19 (3), 529–540.

Simpson, J.H., Vennell, R., Souza, A.J., 2001. The salt fluxes in a tidally - energetic estuary. Estuar. Coast. Shelf Sci. 52 (1), 131–142.

Stanev, E., Brink-Spalink, G., Wolff, J., 2007. Sediment dynamics in tidally dominated environments controlled by transport and turbulence: a case study for the east Frisian Wadden Sea. J. Geophys. Res. 112, C04018 (1-20).

Tian, T., Merico, A., Jian-Su, J., Staneva, J., Wiltshire, K., Wirtz, K., 2009. Importance of resuspended sediment dynamics for the phytoplankton spring bloom in a coastal marine ecosystem. J. Sea Res. 62, 214–228. http://dx.doi.org/10.1016/j.seares.2009.04.001.

Valle-Levinson, A., 2010. Contemporary Issues in Estuarine Physics. Cambriges University Press, New York, p. 315.

Van der Lubbe, J.J.L., Tjallingii, R., Prins, M.A., Brummer, G.A., Jung, S.J.A., Kroon, D., Schneider, R.R., 2014. Sedimentation patterns off the Zambezi River over the last 20,000 years. Mar. Geol. 355, 189–201. http://dx.doi.org/10.1016/j.margeo.2014.05.012.

Zhang, K.Q., Douglas, B.C., Leatherman, S.P., 2004. Global warming and coastal erosion. Clim. Change 64, 41–58.

Zhao, Y., Jones, M.L., Shuter, B.J., Roseman, E.F., 2009. A biophysical model of a Lake Erie Walleye (Sander vitreus) explains interannual variation in recruitment. Can. J. Fish Aquat. Sci. 66, 114–125. http://dx.doi.org/10.1139/F08-188.